

# Combining Embeddings and Fuzzy Time Series for High-Dimensional Time Series Forecasting in Internet of Energy Applications

Hugo Vinicius Bitencourt<sup>a,b</sup>, Luiz Augusto Facury de Souza<sup>b</sup>, Matheus Cascalho dos Santos<sup>b</sup>, Petrônio Cândido de Lima e Silva<sup>c</sup>, Frederico Gadelha Guimarães<sup>b,\*</sup>

<sup>a</sup>Graduate Program in Electrical Engineering, Universidade Federal de Minas Gerais, Belo Horizonte, Brazil

<sup>b</sup>Machine Intelligence and Data Science (MINDS) Laboratory, Federal University of Minas Gerais, Belo Horizonte, Brazil

<sup>c</sup>Federal Institute of Education Science and Technology of Northern Minas Gerais, Januária Campus, Brazil

---

## Abstract

The prediction of residential power usage is essential in assisting a smart grid to manage and preserve energy to ensure efficient use. An accurate energy forecasting at the customer level will reflect directly into efficiency improvements across the power grid system, however forecasting building energy use is a complex task due to many influencing factors, such as meteorological and occupancy patterns. In addition, high-dimensional time series increasingly arise in the Internet of Energy (IoE), given the emergence of multi-sensor environments and the two way communication between energy consumers and the smart grid. Therefore, methods that are capable of computing high-dimensional time series are of great value in smart building and IoE applications. Fuzzy Time Series (FTS) models stand out as data-driven non-parametric models of easy implementation and high accuracy. Unfortunately, the existing FTS models can be unfeasible if all features were used to train the model. We present a new methodology for handling high-dimensional time series, by projecting the original high-dimensional data into a low dimensional embedding space and using multivariate FTS approach in this low dimensional representation. Combining these techniques enables a better representation of the complex content of multivariate time series and more accurate forecasts.

*Keywords:* Multivariate time series, Fuzzy Time Series, Embedding Transformation, Time series forecasting, Smart Buildings, Internet of Energy.

---

## 1. Introduction

We are on the cusp of a new age of ubiquitous networks (i.e. networks available anywhere, anytime) and communication that has transformed corporate, community and personal spheres. Connections are multiplying, creating an entirely new dynamic network - the Internet of Things (IoT). Internet of Things means a global network of interconnected objects (e.g. RFID tags, sensors, actuators, mobile phones) that are uniquely addressable and based on standard communication protocols [1] [2] [3].

The Internet of Things may impact various aspects of everyday life and the behavior of potential users, and popular demand combined with technological advances could drive the widespread diffusion of an IoT that could contribute to economic development. Sensor nodes and actuators distributed throughout homes and offices can make our lives more comfortable, for example: room heating can

be adjusted to our preferences and the weather; domestic incidents can be avoided with appropriate monitoring and alarm systems; and energy can be saved by automatically turning off electrical appliances when they are not needed. Roads can be equipped with tags and sensor nodes that send important information to traffic control centers and transportation vehicles to better direct traffic. Sensors can also be used to monitor water quality, diagnose and treat diseases [4] [5] [6].

The integration of sensor nodes, actuators, smart meters and other components of the electrical grid together with information and communication technology is called the Internet of Energy (IoE). IoE uses the bidirectional flow of energy and information within the electrical grid to gain deep insights into electricity usage and benefit from future actions to increase energy efficiency. IoE is a subcategory of IoT and an indispensable component in the implementation of smart grids [7] [5] [8].

Smart grids can be defined as the modernization of electrical power systems to achieve a fully automated power grid by integrating all connected users. In smart grids, all players (suppliers and consumers) are digitally connected. Smart grid technology promises to make power systems safer, more reliable, more efficient, more flexible and more sustainable. It achieves these goals through the use of IoE

---

\*Corresponding author

*Email addresses:* hugovynicius@ufmg.br (Hugo Vinicius Bitencourt), petronio.candido@ifmg.edu.br (Petrônio Cândido de Lima e Silva), fredericoguimaraes@ufmg.br (Frederico Gadelha Guimarães)

*URL:* <https://minds.eng.ufmg.br/> (Frederico Gadelha Guimarães)

technology in power grids [9].

Smart buildings or smart homes use IoE devices to monitor various building characteristics, analyze the data, and generate insights into usage patterns and trends that can be used to optimize the building environment and operations. The concept of smart homes can be easily extended to all types of buildings such as industrial, commercial and residential buildings [10].

In smart buildings, all digital devices are interconnected to form an IoE network that automates or assists users in various ways, for example, IoE devices monitor home energy consumption and users can control their home electricity usage through bidirectional communication with home appliances [8].

There is a need to add computational intelligence at all levels of the smart grid to mitigate potential uncertainties in the electrical grid. An important feature of smart buildings is the ability to forecast energy consumption, as utilities are expected to learn the patterns of energy consumption and predict demand to make appropriate decisions. A smart learning mechanism enables energy planning strategies that contribute to more efficient use of electricity, higher end-use efficiency, and effective use of electricity infrastructure [11] [12] [13].

The ability to control and improve energy efficiency and predict future demand is imperative for smart buildings. Accurate energy forecasting at the customer level will reflect directly into efficiency improvements across the power grid system, but forecasting building energy use is a complex task due to many influencing factors, such as meteorological and occupancy patterns.

In the context of IoE, an enormous amount of sensor nodes collect sensory data over time for a variety of applications, resulting in a huge amount of continuous data and Big Data streams. The data is continuously recorded from various data sources and each sensor generates a streaming time series, where each dimension represents the measurements recorded by a sensor node, resulting in a high-dimensional time series. Formally, an IoT application with  $M$  sensors generates an  $M$ -dimensional time series. IoT and IoE are one of the most important sources of Big Data, as they rely on connecting a large number of devices to the Internet to continuously report the state of the environment.

In addition, IoE devices may suffer from unavoidable aging effects or faults in their embedded electronics, then many such data may exhibit errors and noise during acquisition and transmission. Furthermore, the physical phenomena to be monitored may also change over time due to seasonality.

In this sense, forecasting methods for high-dimensional time series have become one of the active topics in machine learning researches. Methods capable of handling high-dimensional time series are of great value in IoE applications. The analysis of such datasets presents significant challenges, both from a statistical and numerical perspective.

Fuzzy Time Series (FTS) methods became attractive due to their ease of implementation, low computational cost, predictive accuracy, and model interpretability. However, as the dimensionality of the time series increases, FTS methods significantly lose accuracy and simplicity. Since each variable has its own fuzzy sets and the number of rules in a multivariate FTS model is given by a combination of the fuzzy sets, the number of rules can grow exponentially with the number of variables [14] [15]. Therefore, it is neither practical nor computationally sound to impose all input data on an FTS forecasting model. The challenge then is to design an optimal set of inputs based on their strong correlations with the target output.

To overcome these challenges presented above, we introduce here a new methodology for forecasting high-dimensional time series called  $\gamma$ FTS (Embedding Fuzzy Time Series). We apply a data embedding transformation and use FTS models in a low dimensional, learned continuous representation. Embedding allows us to extract a new feature space that better represents the complex content of multivariate time series data for the subsequent forecasting task. The combination of these techniques enables better representation of the complex content of high-dimensional time series and accurate forecasting.

The  $\gamma$ FTS was tested to solve the problem of energy consumption forecasting of devices in smart buildings. The methodology was used to extract a new feature space that better represents the content of the multivariate time series of energy consumption for the subsequent forecasting task. The embedding methods allow us to extract the relevant information that supports the prediction of the target variable.

The main contributions of our work are:

1. Investigating the potential benefits of a method that combines an embedding transformation and a fuzzy time series forecasting approach for dealing with high-dimensional time series data;
2. We present a new methodology that has great value for IoE applications in smart buildings and can help homeowners reduce their electricity consumption and provide better energy saving strategies;
3. The proposed methodology generates models that are fully readable, transparent, testable and explainable.

The remainder of the work is organized as follows. In section 2 related work, both from the standpoint of application and methodology, is presented. In section 3 the proposed approach is described in detail. Section 4 describes the case studies of three smart building applications used to test our method. The results of the case studies are presented and discussed in section 5. Section 6 concludes the paper.

## 2. Literature Review

In this section, we present the related works, both from the point of view of application and methodology. This section describes Wireless Sensor Networks, presents current methods for energy consumption forecasting in Smart Buildings and defines fuzzy time series and embedding transformation.

### 2.1. Energy Consumption Forecasting

Wireless Sensor Networks (WSN) is a key component of the Internet of Energy and the Internet of Things. WSNs consist of many devices called sensor nodes. Sensor nodes are autonomous, compact, low-power sensors integrated with a low-power embedded CPU, memory, and wireless communication, and may also have local data processing and multi-hop communication [16] [17].

Sensor nodes can be used to detect or monitor a variety of physical parameters or conditions (e.g., humidity, temperature). WSNs offer numerous possibilities for power grids, such as power monitoring, demand-side energy management, coordination of distributed storage, and integration of renewable energy generators.

Wireless Sensor Networks have been used to collect data to analyze the behavior and proper use of energy. Prediction of energy consumption is very important for smart buildings as it helps to reduce power consumption and achieve better energy and cost savings. Forecasting energy consumption allows home and building managers to plan energy use over time, shift energy use to off-peak times, identify goals for energy savings, and make more favorable plans for energy purchases [11] [18].

Smart Buildings is one of the most popular IoE applications that can help increase the energy efficiency of the home. Home appliances can be connected to the internet to help homeowners have better control over their home utility and spending, and can be used in conjunction with meteorological data to predict appliance energy consumption [13] [11].

Forecasting energy consumption in smart buildings is a time series problem consisting of one- or high-dimensional features. These time series usually have seasonal variations and irregular trend components. The data recorded by sensor nodes may also contain missing values, outliers, and uncertainties. Therefore, accurate energy consumption forecasting is a difficult task due to these unpredictable disturbances and noisy data.

Several machine learning models have been used to predict energy consumption using historical data collected from sensor nodes. These techniques have been developed to improve the quality of the power grid and optimise energy utilisation.

Candanedo et al. [19] implemented and evaluated four data-driven predictive models for appliance energy consumption in a low-energy house in Belgium. The authors tested Multiple Linear Regression (MLR), Support Vector

Machine with Radial Kernel (SVM-radial), Random Forest (RF), and Gradient Boosting Machines (GBM). The best model was GBM, which could explain 57% of the variance ( $R^2$ ) and achieved an RMSE of 66.65, a MAE of 35.22 and a MAPE of 38.29% in the testing set when all features were used.

Chammas et al. [20] proposed a Multilayer Perceptron (MLP) with four hidden layers and 512 neurons in each layer to predict the energy consumption of appliances. The MLP model was able to predict 56% of variance with 66.29 of RMSE, 29.55 MAE and 27.96% MAPE in the testing set when all features were used.

Mocanu et al. [18] developed two variants of the Restricted Boltzmann Machines (RBMs) stochastic model for forecasting residential energy consumption, namely the Conditional RBM (CRBM) and the Factored Conditional RBM (FCRBM). The authors compared the two methods with traditional machine learning methods such as Support Vector Machines (SVM), Artificial Neural Networks (ANN) and Recurrent Neural Networks (RNN), testing different time horizons with different time resolutions from one minute to one week. The FCRBM achieved the highest accuracy compared to ANN, RNN, SVM and CRBM. However, only one-dimensional time series were considered.

Recently, several hybrid deep learning models have been proposed. This concept consists of mixing different models with unique technique to address the limitations of a single model to increase the forecasting performance. For example, Convolutional Neural Network is used to extract spatial features and Recurrent Neural Networks is used to model temporal features.

Long Short-Term Memory Network (LSTM) models have been attracting the attention of many researches to perform energy consumption forecasting. Syed et al. [21] proposed a framework consisting of a hybrid stacked bi-directional and uni-directional LSTM with fully connected dense layers and data cleaning process (HSBUFC). The prediction performance of this framework was superior than other hybrid deep learning models such as CNN-LSTM and ConvLSTM.

Kim and Chao [22] integrated Convolutional Neural Network (CNN) with LSTM for forecasting the energy consumption of houses, namely CNN-LSTM. The CNN was used to extract features that affect energy consumption and the LSTM for modeling the temporal information. The hybrid model achieved better performance than LSTM and obtained values of 37.38 and 61.14 for MSE and RMSE, respectively. According to the authors, the main limitation of the hybrid model is the relatively large effort through trial and error to determine the optimal hyperparameters.

Sajjad et al. [23] implemented a hybrid deep learning-based energy forecasting model (CNN-GRU). Their solution uses CNN to extract spatial features from the energy consumption dataset and uses Gated Recurrent Unit (GRU) to exploit its effective gated structure to make en-

ergy consumption forecasting. The results showed that CNN-GRU had improved performance compared to individual forecasting models and the CNN-LSTM model.

Ullah et al. [24] proposed a hybrid deep learning model by integrating CNN with multilayer bidirectional LSTM (M-BLSTM) for short-term power consumption forecasting and compared their results with bidirectional LSTM (BLSTM), LSTM and CNN-LSTM. The prediction result showed that the hybrid model outperforms LSTM, BLSTM and CNN-LSTM.

Munkhdalai et al. [25] presents the AIS-RNN model, which combines RNNs with an adaptive feature selection mechanism to improve forecasting performance. The model consists of two parts: the first model generates contextual importance weights for selecting appropriate features; then, the second model predicts the target variable (i.e., device energy consumption) based on the inputs. The authors compared their model with different machine learning and deep learning models such as LSTM, GRU, and SVM, and the results showed that the AIS-RNN model outperformed the other models.

Parhizkar et al. [26] improved the performance of smart building forecasting models by using PCA to preprocess data and extract key features representing four smart building datasets for the subsequent forecasting task. The authors used five machine learning models (linear regression, support vector regression, regression tree, random forest, and K-nearest neighbours) to predict energy consumption.

## 2.2. Fuzzy Time Series

The foundations of Fuzzy Time Series (FTS) were first proposed by Song and Chissom [27] to deal with ambiguous and imprecise knowledge in time series data. FTS is a representation of time series using fuzzy sets as fundamental components, then conventional time series values are transformed into linguistic time series. Since the introduction of FTS, several categories of FTS methods have been proposed, which are distinguished by their order ( $\Omega$ ) and time variance. The order is the number of time delays (lags) used in modeling the time series. Time variance defines whether the FTS model changes over time [15]. A first order FTS model requires  $y(t-1)$  data to predict  $y(t)$  and a high order FTS model requires  $y(t-1), \dots, y(t-p)$  data to predict  $y(t)$ .

In the training procedure of an FTS model, the Universe of Discourse ( $U$ ) is partitioned into intervals bounded by the known limits of  $Y$ , where  $U = [\min(Y), \max(Y)]$ . For each interval, a fuzzy set  $A_i \in \tilde{A}$  with its own membership function (MF)  $\mu_{A_i} : \mathbb{R} \rightarrow [0, 1]$  is defined, then each fuzzy set is assigned a linguistic value that represents a range of  $U$ . The crisp time series  $Y$  is mapped to the fuzzified time series  $F$ , given the membership values to the fuzzy sets. Temporal patterns corresponding to the number of lags  $\Omega$  are created from  $F$ . Each pattern represents a fuzzy rule called Fuzzy Logical Relationship (FLR) and they are grouped by their same precedents to form a Fuzzy Logical Relationship Group (FLRG). The FLRG form the

rule base which is the final representation of the FTS forecasting model.

Once the FTS model is trained, it can be used to predict new values. The crisp samples  $y(t-\Omega), \dots, y(t-1)$  are mapped to the fuzzified values  $f(t-\Omega), \dots, f(t-1)$ , where  $f(t) = \mu_{A_i}(y(t)), \forall A_i \in \tilde{A}$ , for  $t = 1, \dots, T$ . The rules matching the corresponding input are found. The FLRG whose precedent is equal to the input value is selected and the candidate fuzzy sets in its consequent are applied to estimate the predicted value.

## 2.3. Dimensionality Reduction

There are several approaches in the literature for dealing with high-dimensional data. Some of the main dimensionality reduction (embedding) techniques are feature selection and feature extraction. In feature selection, a subset of the original features is selected. On the other hand, in feature extraction, a set of new features is found by mapping from the existing input variables. The mapping can be either linear or non-linear.

The goal of embedding by feature extraction is to learn a function  $\gamma : \mathbb{R}^M \rightarrow \mathbb{R}^K$  that maps  $M$ -dimensional features measured over  $T$ -time steps into the reduced  $K$ -dimensional feature space with  $K \ll M$ .

There are several feature extraction methods that can be used for different types of data and different requirements. In this paper, we focus on three of them: Principal Component Analysis (PCA) [28], Autoencoder (AE) [29] and Self-organizing maps (SOM) [30].

## 3. Embedding-based Fuzzy Time Series ( $\gamma$ FTS)

A multivariate time series  $Y \in \mathbb{R}^M$  is an extension of the univariate case, containing values of different univariate time-dependent variables. The dimensionality of  $Y$  is given by  $M = |\mathcal{V}|$  and each vector (i.e., the set of variables)  $y(t) \in Y$  carries all variables  $\mathcal{V}_i \in \mathcal{V}$ .

The multivariate FTS model is an extension of several univariate FTS models used to capture the linear or non-linear interdependencies between multiple fuzzy time series. Multivariate FTS forecasting methods can be divided into Multiple Input Single Output (MISO) and Multiple Input Multiple Output (MIMO) methods. The MISO obtains a set of explanatory variables (or exogenous)  $\mathcal{V}_i \in \mathcal{V}$  and only one target variable (or endogenous)  $\mathcal{V}^* \in \mathcal{V}$ , which is the output set, while the MIMO method uses the same input set of variables as the output set.

In this work, we propose a new MISO FTS method, called  $\gamma$ FTS, to handle high-dimensional multivariate time series by applying an embedding transformation, then reducing the dimensionality of the time series and enabling efficient pattern recognition and induction of fuzzy rules.

The  $\gamma$ FTS method is a data-driven and explainable method that is flexible and adaptable for many IoE applications. The proposed approach consists of embedding, training and forecasting procedures. This paper is a substantial extension of the works presented in [31] and [32].

### 3.1. Embedding Procedure

The embedding procedure is responsible for extracting the principal components that better represent the content of the high-dimensional multivariate time series for the subsequent forecasting task.

#### 3.1.1. Principal Component Analysis (PCA)

Principal Component Analysis (PCA) is one of the most popular feature extraction approaches. PCA estimates the cross-correlation among the variables and extracts a reduced set of features, called principal components, which are linearly uncorrelated. The principal components explain the largest possible proportion of the data variance with the constraint that they are orthogonal to all previously extracted features. PCA extracts a reduced data representation that describes a specific total percentage of the data variance.

The PCA embedding procedure consists of the following steps: Starting from the multivariate time series  $Y \in \mathbb{R}^{N \times M}$ , we compute the covariance matrix  $C \in \mathbb{R}^{M \times M}$  and extract the first  $K$  eigenvectors related to the largest eigenvalues. Thus, we obtain the matrix  $Z \in \mathbb{R}^{M \times K}$ , which is used to compute the embedding feature  $\gamma(x) : Z^T \cdot y$  with  $y \in \mathbb{R}^M$ .

#### 3.1.2. Autoencoder (AE)

Autoencoders (AEs) are a special type of artificial neural network whose task is to convert the input into a latent and meaningful representation, that is, to encode the data. The autoencoder was first introduced in [29] as a simple network that attempts to reconstruct the input, and it has been used to solve unsupervised learning and transfer learning problems, as this technique attempts to produce the best possible representation of the input by minimizing the reconstruction error. That is, it decodes back the encoded representation of the input and compares it with the real input [13] [33].

An autoencoder network consists of an encoder layer and a decoder layer connected by one or more hidden layers that transform high-dimensional data into a  $K$ -dimensional representation. The embedding transformation is achieved by exploiting bottleneck features extracted in the hidden layers, and the autoencoder can handle nonlinear correlations between variables.

The AE embedding procedure aims to learn the encoding function  $e : \mathbb{R}^M \rightarrow \mathbb{R}^K$  and the decoding function  $d : \mathbb{R}^K \rightarrow \mathbb{R}^M$ , according to equation

$$(e(\cdot), d(\cdot)) = \arg \min_{e(\cdot), d(\cdot)} \|Y - d(e(Y))\|^2 \quad (1)$$

We have used the encoding function  $e$  as a direct embedding function  $\gamma$  for the high-dimensional time series  $Y \in \mathbb{R}^M$ , such that

$$\gamma(Y) = e(Y) \quad (2)$$

#### 3.1.3. Self-organizing maps (SOM)

Self-organizing maps (SOM) is an unsupervised learning approach that projects the original continuous space  $\mathcal{D} \subseteq \mathbb{R}^M$  into a finite, discrete  $K$ -dimensional array  $W$  named grid, where each cell  $w_i \in W$  corresponds to a point of  $\mathcal{D}$ , and each dimension  $K$  has a fixed length  $L \in \mathbb{N}^+$ . The embedding space  $\mathcal{E}$  of the map is composed of the  $K$  coordinates of the grid, then its dimensions are finite, discrete and positive.

In the training procedure of a SOM model, the grid  $W$  is gradually approximated to the topology of the original space by fitting the cells  $w_i$  to the values of this space and their neighbor values. The training process is unsupervised and iterative. The SOM embedding procedure performs a nearest neighbor search on the grid  $W$  to find the coordinates of the best matching cell. Formally, the embedding process transforms the input  $y \in Y$  into the  $k$ -dimensional embedding space  $y_\gamma(t)$

The training procedure is shown in Algorithm 1, where  $T$  is the length of the training data,  $\alpha$  is the learning rate,  $\sigma$  is the neighborhood radius,  $d : \mathbb{R}^n \times \mathbb{R}^n \rightarrow \mathbb{R}^+$  is the Euclidean distance metric, and  $f(i, u, \sigma, \alpha)$  is the Gaussian neighborhood function given by (3). The parameters  $\alpha$  and  $\sigma$  control the adaption velocity during training and the amplitude of the neighbor cells affected when  $W$  is updated (using the Gaussian neighborhood function  $f$ ), and both parameters are monotonically decreased during the training loop.

$$f(i, u, \sigma, \alpha) = \alpha \cdot \exp\left(-\frac{\|w_i - w_u\|^2}{2\sigma^2}\right) \quad (3)$$

---

#### Algorithm 1: SOM Training

---

**input** :  $Y, k, L, \alpha_0, \sigma_0$

**output**:  $W$

Create the grid  $W$  with  $k$  dimensions and each dimension with  $L$  cells, where each cell  $w_i \in W$  is a  $1 \times n$  vector;

Initialize each  $w_i \in W$  with random values;

**for**  $t \leftarrow 1$  **to**  $T$  **do**

    Get an instance  $y(t) \in Y$ ;

    Find the closest cell  $w_u$  to  $y(t)$  such that

$w_u = \arg \min_{w_i} d(y(t), w_i) \forall w_i \in W$ ;

**foreach**  $w_i \in W$  **do**

        |  $w_i \leftarrow w_i + f(i, u, \sigma_t, \alpha_t) \cdot (y(t) - w_i)$

**end**

    Decrease the neighborhood radius  $\sigma$  such that

$\sigma_t \leftarrow \sigma_0 \left(\frac{\sigma_t}{\sigma_0}\right)^{\frac{t}{T}}$

    Decrease the learning rate  $\alpha$  such that

$\alpha_t \leftarrow \alpha_0 \left(\frac{\alpha_t}{\alpha_0}\right)^{\frac{t}{T}}$

**end**

---

The SOM training procedure is an iterative and unsupervised procedure that gradually approximates the grid  $W$  to the topology of the original space by fitting the cells  $w_i$  to the values of this space and their neighbor values.

The SOM embedding function is much simpler than the training procedure and simply performs a nearest neighbour search on the grid  $W$  and returns the coordinates of the best matching cell. In this way, the map transforms the input  $y \in Y$  into the  $k$ -dimensional embedding vector  $y_\gamma(t)$ . The SOM Embedding function is presented in Algorithm 2.

---

**Algorithm 2: SOM Embedding**

---

**input** :  $y \in Y, W$

**output**:  $y_\gamma$

Find the closest cell  $w_u$  to  $y(t)$  such that

$$w_u = \arg \min_{w_i} d(y(t), w_i) \forall w_i \in W$$

$y_\gamma \leftarrow$  get map coordinates of  $w_u$  in  $W$ ;

---

### 3.2. Training Procedure

The training procedure shown in Figure 1 creates a multivariate FTS model  $\mathcal{M}$  that captures all the information in the embedding data. Let the embedding multivariate time series  $Y_\gamma \in \mathbb{R}^K$  and its individual instances  $y_\gamma(t) \in Y_\gamma$  for  $t = 0, 1, \dots, T$  and the number of fuzzy sets  $\kappa$ . The training procedure consists of the following steps:

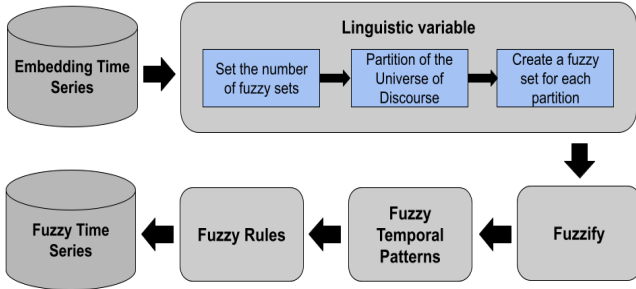


Figure 1:  $\gamma$ FTS Training procedure

- Partitioning**: define  $U_{\mathcal{V}_\gamma} = [lb, ub]$ , where  $lb = \min(Y_\gamma) - D_1$  and  $ub = \max(Y_\gamma) + D_2$ , with  $D_1 = r \times |\min(Y_\gamma)|$  and  $D_2 = r \times |\max(Y_\gamma)|$ ,  $0 < r < 1$ . We extrapolate the known bounds of the variables  $\mathcal{V}_{\gamma_i}$  as a security margin.
- Defining the linguistic variable**: split  $U_{\mathcal{V}_\gamma}$  in  $\kappa_i$  (i.e. number of fuzzy sets) overlapping intervals  $U_j$  with midpoints  $c_j$  for  $j = 0, 1, 2, \dots, \kappa_i$ . For each interval  $U_j \in U_{\mathcal{V}_\gamma}$  create an overlapping fuzzy set  $\mathcal{A}_j^{\mathcal{V}_i}$  with the membership function  $\mu_{\mathcal{A}_j^{\mathcal{V}_i}}$  and generate a variable  $\mathcal{V}_{\gamma_i}$  for the dimension  $i$  and a linguistic variable  $\tilde{\mathcal{V}}_{\gamma_i} \in \tilde{\mathcal{V}}_\gamma$ . Each fuzzy set  $\mathcal{A}_j^{\mathcal{V}_i}$  represents a linguistic variable  $\tilde{\mathcal{V}}_{\gamma_i}$ .
- Fuzzification**: the embedding time series  $Y_\gamma$  is then transformed into a fuzzy time series  $F_\gamma$ . Each data point  $f_\gamma(t) \in F_\gamma$  is an  $n \times \kappa$  array with the fuzzified

values with respect to the linguistic variable, where the fuzzy membership is predefined as follows

$$f(t) \leftarrow \left\{ \mathcal{A}_j^{\mathcal{V}_i} \mid \mu_{\mathcal{A}_j^{\mathcal{V}_i}}(Y_\gamma(t)^i) > 0 \right\} \quad (4)$$

- Generate the temporal patterns**: generate temporal patterns with the format  $\mathcal{A}_j^{\mathcal{V}_0}, \dots, \mathcal{A}_j^{\mathcal{V}_n} \rightarrow \mathcal{A}_j^{\mathcal{V}^*}$ , where the precedent or LHS (left hand side) is  $f_\gamma(t) = \mathcal{A}_j^{\mathcal{V}_i}$  and the consequent or RHS (right hand side) is the target variable such that  $f_\gamma(t+1) = \mathcal{A}_j^{\mathcal{V}^*}$ . Both LHS and RHS are related to  $\mathcal{A}_j^{\mathcal{V}_i}$  with maximum membership.
- Generate the rule base**: finally, each pattern represents a fuzzy rule and they are grouped by their same precedents, creating a fuzzy rule  $r$  with the format  $LHS \rightarrow RHS$ . Each fuzzy rule represents the set of possibilities with may happen on time  $t+1$  when a certain precedent is identified on previous lag.

### 3.3. Forecasting Procedure

The forecasting procedure, shown in Figure 2, finds the rules that match a given fuzzified input and uses them to compute a numerical prediction using the fuzzy sets. This procedure aims to estimate  $y(t+1)$  for the endogenous variable  $\mathcal{V}^* \in \mathbb{R}$ , given an input sample  $y(t)_{\gamma_i}$  and using the fuzzy rules of the FTS model  $\mathcal{M}$ .

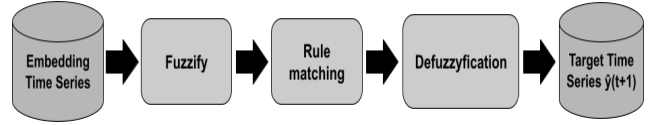


Figure 2:  $\gamma$ FTS Testing procedure

Given the embedding multivariate time series  $Y_\gamma \in \mathbb{R}^K$  and its individual instances  $y_\gamma(t) \in Y_\gamma$  for  $t = 0, 1, \dots, T$ , the following steps are taken to forecast  $\hat{y}(t+1)$ .

- Fuzzification**: for each variable  $\mathcal{V}_i \in \mathcal{V}$ , we fuzzify the embedding data according to equation 4.
- Rule matching**: select  $r$  fuzzy rules whether any fuzzy set of  $f(t)$  is equal to LHS. The rule fuzzy membership grade is computed using the minimum function T-norm as follows

$$\mu_q = \bigcap_{j \in \tilde{\mathcal{V}}_i; i \in \mathcal{V}} \mu_j^i \quad (5)$$

- Rule mean points**: for each rule  $q$ , we compute the mean point  $mp_q$  of the endogenous variable  $\mathcal{V}^*$  according the following equation

$$mp_q = \sum_{j \in \tilde{\mathcal{V}}_i^*} c_j \quad (6)$$

where  $c_j$  is the  $c$  parameter of the membership function from the fuzzy sets.

4. **Defuzzification:** finally, the predicted value  $\hat{y}(t+1)$  is obtained as the weighted sum of the rule midpoints by their membership grades  $\mu_{A_j}$ , according to equation:

$$\hat{y}(t+1) = \sum_{q \in r} \mu_q \cdot mp_q \quad (7)$$

### 3.4. Embedding Weighted Multivariate Fuzzy Time Series ( $\gamma$ WMVFTS)

To demonstrate our proposed method  $\gamma$ FTS, we extend the Weighted Multivariate Fuzzy Time Series (WMVFTS) method [34] to enable it for high-dimensional time series (i.e.  $\gamma$ WMVFTS). The WMVFTS method is a weighted and rule-based MISO first-order multivariate method that allows individual partitioning schemes for each variable. The training procedure can be easily distributed in network clusters and its knowledge base is easy to understand and verify.

We used the embedding transformation presented in section 3.1 to reduce the dimensionality of the time series and enable efficient pattern recognition and induction of fuzzy rules. WMVFTS combined with PCA, AE and SOM are referred to as PCA-WMVFTS, AE-WMVFTS and SOM-WMVFTS, respectively.

The training procedure of  $\gamma$ WMVFTS model is presented in Algorithm 3 and illustrated in Figure 3. In the **Generate the rule base** step, we create fuzzy rules  $r$  with the format  $LHS \rightarrow w \cdot RHS$ , where  $w = |\mathcal{A}_j^{\mathcal{V}_i}|/|RHS|$  which are normalized frequencies of each temporal pattern (i.e. weights) according to equation

$$w_i = \frac{\#\mathcal{A}_j^{\mathcal{V}_i^*}}{\#RHS} \quad \forall \mathcal{A}_j^{\mathcal{V}_i^*} \in RHS \quad (8)$$

where  $\#\mathcal{A}$  is the number of occurrences of  $\mathcal{A}_i$  on temporal patterns with the same LHS and  $\#RHS$  is the total number of temporal patterns with the same precedent LHS. The other steps remain the same as described in Section 3.2.

Algorithm 4 shows the forecasting procedure of the  $\gamma$ WMVFTS model. In **Rule mean points** step, for each rule  $q$ , we compute the mean point  $mp_q$  of the endogenous variable  $\mathcal{V}^*$  as follows

$$mp_q = \sum_{j \in \tilde{\mathcal{V}}_i^*} w_j \cdot c_j \quad (9)$$

where  $w_j$  is the weights calculated according to 8. The other steps remain the same as presented in Section 3.3.

## 4. Experiments

Several experiments have been conducted to obtain highly accurate energy forecasting in smart buildings using the proposed methodology. We compare the performance of our proposed models with the baseline models and state-of-the-art forecasting models proposed in the literature.

---

### Algorithm 3: $\gamma$ WMVFTS Training

---

**input** : A multivariate time series  $Y$ , number of instances  $N$ , number of dimensions  $K$ , number of fuzzy sets  $\kappa$   
**output**: the linguistic variable  $\tilde{\mathcal{V}}$ , the rule set  $\mathcal{R}$   
**foreach**  $y(t) \in Y$  **do**  
     $y_\gamma(t) \leftarrow$  Embedding Procedure( $y(t)$ ,  $K$ );  
     $Y_\gamma \leftarrow y_\gamma(t)$   
**end**  
**for**  $i \leftarrow 1 \dots k$  **do**  
     $u \leftarrow$  Split  $UoD$  in  $\kappa$  overlapping intervals;  
     $\mathcal{V}_i \leftarrow$  Create a variable for the dimension  $i$ ;  
     $\tilde{\mathcal{V}} \leftarrow$  Create an empty linguistic variable for  $\mathcal{V}_i$ ;  
    **for**  $j \leftarrow 1 \dots N_i$  **do**  
         $\mathcal{A}_j^{\mathcal{V}_i} \leftarrow$  Create a fuzzy set with the interval  $u_j$  with membership function  $\mu_{\mathcal{V}_i}$ ;  
         $\tilde{\mathcal{V}} \leftarrow \mathcal{A}_j^{\mathcal{V}_i}$ ;  
    **end**  
**end**  
 $F \leftarrow$  Create empty fuzzified data;  
**foreach**  $y_\mathcal{E}(t) \in Y_\mathcal{E}$  **do**  
     $f(t) \leftarrow \{ \mathcal{A}_j^{\mathcal{V}_i} \mid \mu_{\mathcal{A}_j^{\mathcal{V}_i}}(y_\mathcal{E}(t)^i) > 0 \}$  for all fuzzy sets  
     $\mathcal{A}_j^{\mathcal{V}_i} \in \tilde{\mathcal{V}}$  and all variables  $\mathcal{V}_i$ ;  
     $F \leftarrow f(t)$ ;  
**end**  
 $\mathcal{R} \leftarrow$  Create an empty set of rules ;  
**foreach**  $f(t), f(t+1) \in F$  **do**  
    **foreach** fuzzy set  $LHS \in f(t)$  **do**  
         $RHS \leftarrow$  all fuzzy sets  $\mathcal{A}_j^{\mathcal{V}_i}$  in  $f(t+1)$  with weight  $w = |\mathcal{A}_j^{\mathcal{V}_i}|/|RHS|$ ;  
         $r \leftarrow$  Create rule  $LHS \rightarrow RHS$ ;  
        **if**  $r$  does not exist in  $\mathcal{R}$  **then**  
             $\mathcal{R} \leftarrow r$ ;  
        **end**  
    **end**  
**end**

---

This section includes the description of the case of studies, the methodology of the experiments, the evaluation metrics, the description of the baseline model, the optimization of the hyperparameters, the computational experiments and the reproducibility.

#### 4.1. Case studies

An important application of IoE in smart buildings is monitoring the energy consumption of devices. This importance stems from the fact that proper monitoring of energy appliances can reduce power consumption and provide better energy and cost savings. In addition, energy forecasting at the customer level will reflect directly into efficiency improvements across the power grid.

As an example of the approach presented here, we evaluate the proposed methodology on three datasets presented below. The input data of each dataset was refined before training our  $\gamma$ WMVFTS models. Therefore, we employ data pre-processing strategies to remove outliers and

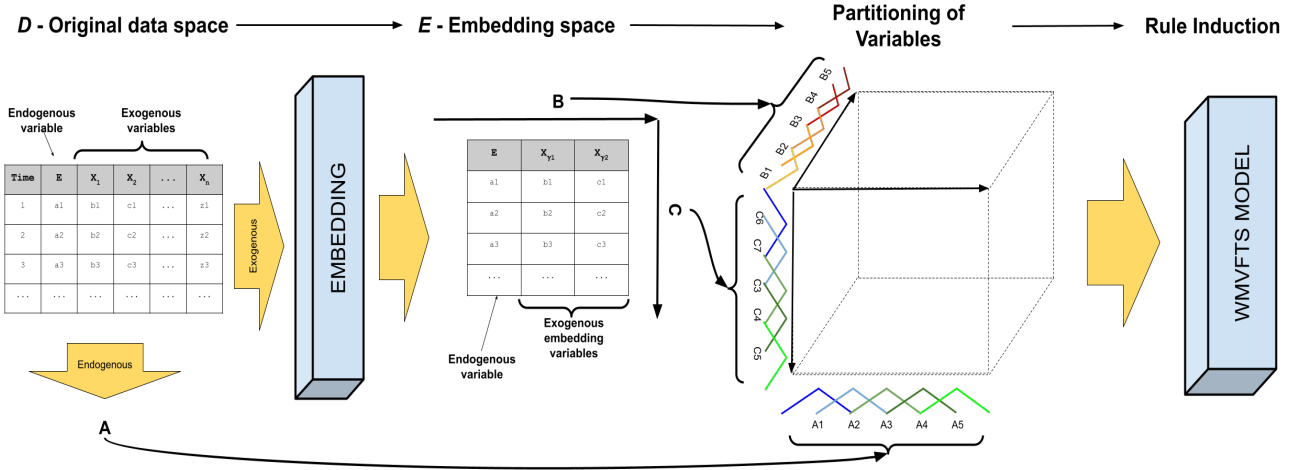


Figure 3:  $\gamma$ WMVFTS training for number of dimensions  $k = 2$  and number of fuzzy sets  $\kappa = 5$

#### Algorithm 4: $\gamma$ WMVFTS Forecasting

**input** : A sample  $y(t)$ , the dimensions  $K$ , the linguistic variable  $\tilde{\mathcal{V}}$ , the rule set  $\mathcal{R}$   
**output**: target forecasting value  $\hat{y}(t+1)$   
 $y_\gamma(t) \leftarrow \text{Embedding Procedure}(y(t), K)$ ;  
 $f(t) \leftarrow \{A_j^{\mathcal{V}_i} \mid \mu_{A_j^{\mathcal{V}_i}}(y_\gamma(t)^i) > 0\}$  for all fuzzy sets  
 $A_j^{\mathcal{V}_i} \in \tilde{\mathcal{V}}$  and all variables  $\mathcal{V}_i$ ;  
 $\mathcal{R}_{fired} \leftarrow$  Create an empty set of rules;  
 $\mu \leftarrow$  Create the empty vector of activation of each rule;  
**foreach**  $r \in \mathcal{R}$  **do**  
  **if** any fuzzy set of  $f(t)$  is equal to  $r_{LHS}$  **then**  
  |  $\mathcal{R}_{fired} \leftarrow r$ ;  
  **end**  
**end**  
**foreach**  $r \in \mathcal{R}_{fired}$  **do**  
   $mp_r \leftarrow \sum_{A_j^{\mathcal{V}_i} \in r_{RHS}} w_i \cdot mp_i$  where  $w_i$  is the weight  
  and  $mp_i$  is the midpoint of the fuzzy set;  
   $\mu_r \leftarrow \prod_{A_j^{\mathcal{V}_i} \in r_{LHS}} \mu_{A_j^{\mathcal{V}_i}}(y(t))$   
**end**  
 $\hat{y}(t+1) = \frac{\sum_{r \in \mathcal{R}_{fired}} \mu_r \cdot mp_r}{\sum_{r \in \mathcal{R}_{fired}} \mu_r}$

missing values on datasets.

##### 4.1.1. UCI Appliances Energy Consumption (AEC-DS)

The ‘‘UCI Appliances energy prediction’’ dataset [35] includes measurements of temperature and humidity collected from a WSN, weather information from a nearby Weather Station, and recorded energy consumption from appliances and lighting fixtures. The energy appliances data were obtained by taking continuous measurements (every 10 minutes) in a low-energy house in Belgium over a period of 137 days between January 11, 2016 and May 27, 2016 (approximately 4.5 months). The dataset con-

tains 19,735 instances, including 26 explanatory variables and 1 temporal variable (date/time). Table 1 shows all variables.

Table 1: UCI Appliances Energy Consumption Dataset (AEC-DS)

Variables	Description
Appliances	Appliances energy consumption
lights	Light energy consumption
RH.1	Humidity in kitchen area
T2	Temperature in living room area
RH.2	Humidity in living room area
T3	Temperature in laundry room area
RH.3	Humidity in laundry room area
T4	Temperature in office room
RH.4	Humidity in office room
T5	Temperature in bathroom
RH.5	Humidity in bathroom
T6	Temperature outside the building
RH.6	Humidity outside the building
T7	Temperature in ironing room
RH.7	Humidity in ironing room
T8	Temperature in teenager room 2
RH.8	Humidity in teenager room 2
T9	Temperature in parents room
RH.9	Humidity in parents room
T_out	Temperature outside
Press_mm_hg	Pressure
RH_out	Humidity outside
Windspeed	Wind Speed
Visibility	Visibility
Tdewpoint	Dew Point
date	Date time stamp

The appliances energy consumption (Wh) measured is the focus of our analysis, then it was chosen as the target variable (endogenous variable)  $\mathcal{V}^*$  and the set of explanatory variables (exogenous variable)  $\mathcal{V}$  is composed of 24



variables.

#### 4.1.2. UCI Household Power Consumption (HPC-DS)

The “UCI Individual household electric power consumption” dataset [35] contains electricity consumption data from a residential house in France. Electricity consumption was collected by continuous measurements over a four-year period from December 2006 to November 2010 with a resolution of one minute. In this work, in some experiments we changed the time resolution of this dataset, growing it to 30 minutes. The dataset consists of 2,075,259 instances and 12 variables, including 7 explanatory variables and 2 temporal variables. A total of 25,979 missing values were removed in pre-processing. Submetering indicate electricity consumption in the kitchen, laundry room, and for the air conditioner and electric water heater. Table 2 shows all variables.

The focus of our analysis is the measured global active power (kW), which we have chosen as the endogenous variable  $\mathcal{V}^*$  and the set of exogenous variables  $\mathcal{V}$  is composed of the past values of six variables.

Table 2: UCI Household Power Consumption Dataset (HPC-DS)

Variables	Description
date	Date
time	time
global_active_power	global active power
global_reactive_power	global reactive power
voltage	averaged voltage
global_intensity	global current intensity
sub_metering_1	energy sub-metering No. 1.
sub_metering_2	energy sub-metering No. 2.
sub_metering_3	energy sub-metering No. 3. .

#### 4.1.3. Kaggle Smart Home with Weather Information Dataset (SHWI-DS)

The “Kaggle Smart home with Weather Information” [36] is a public dataset of IoE devices for smart buildings with weather capabilities. The dataset contains home appliance consumption in kW and weather data from January 2016 to December 2016 with a frequency of 1 minute (in this work, we changed the time resolution to 10 minutes). The dataset contains 500,910 instances and 29 variables, including 18 electricity data features, 10 weather data features, and 1 temporal data feature. Table 3 shows all variables.

The total measured energy consumption (kW) is our target variable  $\mathcal{V}^*$  and the set of exogenous variables  $\mathcal{V}$  is composed of the remaining variables.

#### 4.2. Experiments Methodology

We separate 75% of the data for the training set and 25% for testing and use sliding window cross-validation in the computational experiments. The sliding window is a re-sampling technique based on splitting the data set into

Table 3: Kaggle Smart Home with Weather Information Dataset (SHWI-DS)

Variables	Description
use	Total energy consumption
gen	Total energy generated by solar
Dishwasher	Energy consumed by the dishwasher
Furnace 1	Energy consumed by furnace 1
Furnace 2	Energy consumed by furnace 2
Home office	Energy consumed in home office
Fridge	Energy consumed by fridge
Wine cellar	Energy consumed by wine cellar
Garage door	Energy consumed by garage door
Kitchen 12	Energy consumed in kitchen 1
Kitchen 14	Energy consumed in kitchen 2
Kitchen 38	Energy consumed in kitchen 3
Barn	Energy consumed by barn
Well	Energy consumed by well
Microwave	Energy consumed by microwave
Living room	Energy consumed in living room
Solar	Solar power generation
temperature	Temperature
humidity	Humidity
visibility	Visibility
apparentTemperature	Apparent Temperature
pressure	Pressure
windSpeed	Wind Speed
windBearing	Wind Direction
dewPoint	Dew Point
precipProbability	Precipitation Probability
time	Date time stamp

multiple training and testing subsets. The overall forecasting accuracy is obtained by considering the metric measures over all test subsets. Figure 4 shows cross-validation with sliding window.

The number of instances  $N$  of each dataset was divided into 30 data windows with  $N_{test}$  instances. For each window, we train the forecasting models using the training set, apply the model to the test set, and compute the prediction metrics over the test set. So for each model, there are 30 experiments and we evaluate the performance of the proposed method using the average error value measured in all the windows used for forecasting in the experiments. The performance metrics are described below.

##### 4.2.1. Performance metrics

In order to assess the accuracy of each model, the statistical metrics below were analyzed. Let  $\hat{y}_i$  be the predicted values at the point of interest at time  $t$ ,  $y_i$  the observed values and  $N$  the length of the dataset.

- Root Mean Squared Error (RMSE), defined by equation 10. It shows how accurate the forecasting model is, as it compares the difference between the predicted value and the real value (error), returning the

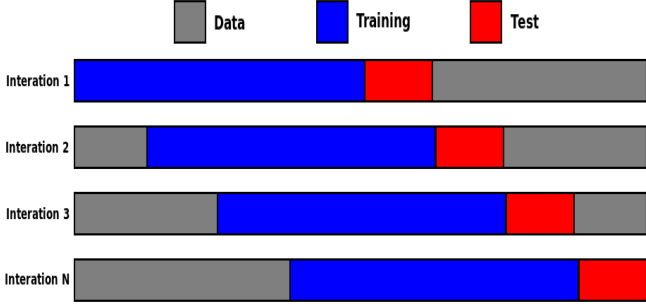


Figure 4: Schematic of the sliding window cross-validation.

standard deviation of this difference.

$$RMSE = \sqrt{\frac{\sum_{i=1}^N (y_i - \hat{y}_i)^2}{N}} \quad (10)$$

- Mean Absolute Percentage Error (MAPE), defined by equation 11. Shows accuracy in terms of percentage error.

$$MAPE = \frac{1}{N} \sum_{i=1}^N \left| \frac{y_i - \hat{y}_i}{y_i} \right| \quad (11)$$

- Mean Absolute Error (MAE), defined by equation. It demonstrates the percentage difference between predicted values.

$$MAE = \frac{1}{N} \sum_{i=1}^N |y_i - \hat{y}_i| \quad (12)$$

- Symmetric Mean Absolute Percentage Error (SMAPE), defined by equation

$$SMAPE = \frac{1}{N} \sum_{i=1}^N \left| \frac{y_i - \hat{y}_i}{|\hat{y}_i| + |y_i|} \right| \quad (13)$$

In addition to the performance evaluation metrics presented above, we evaluate the performance of our proposed methodology using the Skill Score Index. The skill score defines the difference between the forecast and the reference forecast:

$$SkillScore = 1 - \frac{M_F}{M_R} \quad (14)$$

where  $M_F$  refers to the value of the metric for the forecasting method and  $M_R$  is the value of the metric for the reference method. The Skill Score can be used not only to compare with a naive model, but also to compare different forecasting methods with each other [37]. For example, a skill score of 0.50 indicates a 50% improvement in accuracy over the competing model. A negative score indicates worse performance than the competitor model.

### 4.3. Hyperparameters

This section is about finding the right combination of hyperparameters values for Autoencoder and SOM that help us find either the minimum error or the maximum accuracy.

To find the best configuration for embedding with Autoencoder, we empirically tested seven different hyperparameters: Epochs, Stack Size, Optimizer, Learning Rate, Kernel Initializer, Number of Neurons, and Activation Function of Neurons. Each of these hyperparameters was evaluated in a two-layer AutoEncoder architecture with a  $l1$  regularizer in the first layer of both the encoder and the decoder.

In relation to SOM, we also empirically tested the learning rate, epochs, and grid size (i.e. the maximum value of each data in the projected dataset). In addition, the initial neighborhood radius used for all experiments was 12.5.

Since the initialization of the weights is random, the results may be slightly different each time the program is run for both algorithms. Therefore, the mean RMSE and MAPE values of 10 forecast iterations were registered for each hyperparameter to compute a better approximation of each value.

Table 4 shows the values tested for each hyperparameter with autoencoder and the values that obtained the best result are shown in boldface. Table 5 show tested and final (boldface) hyperparameters for SOM.

Table 4: Hyperparameters tested for the AutoEncoder. The best configuration is shown in boldface.

Hyperparameter	Values
Epochs	10, <b>50</b> , 100
Batch Size	10, 20, <b>40</b> , 60, 80, 100
Optimizer	Adam, SGD, RMSprop, AdaDelta, <b>AdaGrad</b> , AdaMax, NAdam
Learning Rate	0.001, 0.01, <b>0.1</b> , 0.2, 0.3
Kernel Initializer	leCun Uniform, <b>Normal</b> , Glorot Normal, Glorot Uniform, He Normal, He Uniform
Neurons	10, 15, 20, 30, 40, <b>50</b> , 100
Activation	Linear, Softmax, Softplus, <b>Softsign</b> , Tanh, Sigmoid, Hard Sigmoid

Table 5: Hyperparameters tested for the SOM. The best configuration found is shown in boldface.

Hyperparameter	Values
Epochs	<b>70</b> , 80, 90, 100
Learning Rate	<b>0.00001</b> , 0.001, 0.01, 0.1,
Grid Size	<b>20</b> , 30, 50, 100

### 4.4. Baseline models

We compared the performance of our proposed approach with the following baseline models: SARIMAX,

PCA-SARIMAX, LSTM and persistence (naive) model, which is a reference technique that assumes that  $y(t)$  equals  $y(t - 1)$ .

The SARIMAX( $p, d, q$ )( $P, D, Q$ ) model (Seasonal Auto Regressive Integrated Moving Average with eXogenous variables) is an extension of SARIMA (seasonal ARIMA) with the possibility of integrating explanatory variables, where  $p, d, q$  and  $P, D, Q$  are non-negative integers related to the polynomial order of the autoregressive (AR), integrated (I), and moving average (MA) non-seasonal and seasonal components, respectively.

The selection of seasonal ( $P, D, Q$ ) and non-seasonal ( $p, d, q$ ) components was based on the Akaike Information Criterion (AIC) using the `auto.arima` function from the `pmдарima` library [38]. `auto.arima` performs a grid search over multiples values of seasonal ( $P, D, Q$ ) and non-seasonal ( $p, d, q$ ) and returns the model with the lower AIC value. We also analysed the autocorrelation (ACF) and partial autocorrelation (PACF) plots to define the seasonal and non-seasonal components. Table 6 shows the values used in each dataset and the input data was normalized before model training, but the forecast error was computed based on actual energy consumption value.

Table 6: Seasonal and non-seasonal components used on SARIMAX model

Dataset	SARIMAX( $p,d,q$ )( $P,D,Q,m$ )
AEC-DS	(0,0,1)(0,1,1,7)
HPC-DS	(1,0,1)(1,1,1,7)
SHWI-DS	(0,0,1)(0,1,1,7)

Using the PCA algorithm presented in Section 3.1.1, we transform  $M$  features of each dataset into  $K = 2$  features and apply the SARIMAX model (henceforth called PCA-SARIMAX) described above. Seasonal and non-seasonal components were selected based on the  $K$  dimensions, and Table 7 shows the values used in each dataset.

Table 7: Seasonal and non-seasonal components used on PCA-SARIMAX model

Dataset	SARIMAX( $p,d,q$ )( $P,D,Q,m$ )
AEC-DS	(1,0,0)(1,0,0,7)
HPC-DS	(1,0,1)(1,1,1,7)
SHWI-DS	(1,0,0)(2,0,1,7)

A Long Short-Term Memory [39] is a recurrent neural network capable of learning to represent large datasets, which makes it extremely useful for applications such as time series forecasting. The LSTM architecture used consists of three layers and kernel regularizers, and we used the configuration of hyperparameters shown in Table 8 for all datasets. These hyperparameters were chosen using hyperopt [40], which is a library designed for hyperparameter

tuning. In other words, it searches for the hyperparameters that provide the minimum loss. Several combinations were tested and we used the best one as baseline.

Since the neural networks are sensitive to diverse data, we normalized the input data before training the LSTM model, but the forecast error was calculated based on the actual energy consumption.

Table 8: LSTM Hyperparameters

Hyperparameter	Value
Neurons	[50,30,10]
Activation	ReLU
Optimizer	ADAM
Batch Size	10
Epochs	70
Loss Function	MSE

#### 4.5. Computational Experiments and Reproducibility

All proposed  $\gamma$ WMVFTS models were implemented and tested using the programming language Python 3, and the open-source pyFSTS [41] and Scikit-Learn [42] libraries. The baseline models were implemented using Python 3, and the following open-sources libraries: Keras [43], Tensorflow [44] and StatsModels [45].

To promote the transparency and the reproducibility of results, all proposed models are available at open-source pyFSTS.

## 5. Results

This section presents the experimental results of our proposed models over several forecasting models tested on the AEC-DS, HPC-DS, and SHWI-DS datasets. First, we present the forecast performance of PCA-WMVFTS and AE-WMVFTS over different configurations of  $K$  dimensions and the partitioning of the target variable (i.e. number of fuzzy sets), comparing a linear embedding algorithm with a nonlinear embedding algorithm. Second, we compare the forecast results of our models with the baseline models described in Section 4.4. Third, we compare the performance of our proposed models with several state-of-the-art forecasting models proposed in the literature. Finally, we present a discussion about the parsimony, computational cost and explainability of our proposed methodology.

#### 5.1. Embedding dimensions and number of fuzzy sets

Tables 9, 10 and 11 present the model performance of PCA-WMVFTS and AE-WMVFTS models over a varying number of  $K$  dimensions and  $\kappa$  number of fuzzy sets on datasets AEC-DS, SHWI-DS, and HPC-DS, respectively. The main hyperparameters of the proposed models are the embedding dimension  $K$  and the number of fuzzy sets  $\kappa$ ,

Table 9: PCA-WMVFTS and AE-WMVFTS model performance with different number of  $K$  dimensions (DIM) and number of fuzzy sets (FS) on AEC-DS

		PCA-WMVFTS				AE-WMVFTS			
DIM	FS	RMSE(Wh)	MAE(Wh)	MAPE(%)	SMAPE(%)	RMSE(Wh)	MAE(Wh)	MAPE(%)	SMAPE(%)
2	10	28.957	20.513	29.81	11.582	31.388	23.469	36.062	13.352
	20	17.095	8.683	11.233	4.694	18.793	10.325	14.334	5.89
	30	9.859	4.326	5.212	2.225	12.295	5.714	6.965	2.934
	40	8.585	2.897	3.163	1.285	10.802	4.315	5.063	2.113
	50	<b>5.457</b>	<b>2.05</b>	<b>1.758</b>	<b>0.746</b>	<b>5.516</b>	<b>2.493</b>	<b>2.405</b>	<b>1.107</b>
3	10	16.988	9.556	14.354	5.401	20.251	12.914	19.361	7.428
	20	4.117	2.158	2.166	0.973	9.689	4.09	4.433	1.821
	30	2.06	1.316	0.671	0.298	2.948	1.636	1.005	0.448
	40	0.996	1.072	0.286	0.131	1.609	1.239	0.601	0.28
	50	<b>0.348</b>	<b>0.962</b>	<b>0.107</b>	<b>0.049</b>	<b>0.781</b>	<b>1.029</b>	<b>0.216</b>	<b>0.103</b>
4	10	10.451	4.4	6.11	2.069	11.872	5.782	7.356	2.968
	20	1.495	1.182	0.507	0.215	1.663	1.304	0.549	0.255
	30	0.415	0.958	0.093	0.041	0.792	1.033	0.201	0.086
	40	0.187	0.935	0.061	0.026	0.137	0.925	0.044	0.019
	50	<b>0.083</b>	<b>0.92</b>	<b>0.035</b>	<b>0.015</b>	<b>0.078</b>	<b>0.917</b>	<b>0.033</b>	<b>0.013</b>
5	10	6.006	2.561	3.086	0.872	5.314	3.003	2.921	1.209
	20	0.587	0.991	0.157	0.061	0.407	0.988	0.124	0.059
	30	0.071	0.917	0.028	0.011	0.099	0.922	0.039	0.017
	40	0.042	0.913	0.024	0.009	0.047	0.913	0.025	0.01
	50	<b>0.044</b>	<b>0.913</b>	<b>0.024</b>	<b>0.009</b>	<b>0.069</b>	<b>0.915</b>	<b>0.026</b>	<b>0.01</b>
6	10	2.697	1.566	1.301	0.452	2.858	1.549	0.902	0.418
	20	0.11	0.923	0.037	0.016	0.145	0.93	0.047	0.02
	30	0.051	0.914	0.025	0.01	0.067	0.916	0.029	0.012
	40	0.041	0.913	0.024	0.009	0.041	0.913	0.024	0.009
	50	<b>0.039</b>	<b>0.912</b>	<b>0.024</b>	<b>0.009</b>	<b>0.039</b>	<b>0.912</b>	<b>0.024</b>	<b>0.009</b>

then we can improve the performance of our models by just increasing the values of these hyperparameters. The performance metrics were computed in the testing set.

Regarding to AEC-DS, PCA-WMVFTS is just slightly superior than AE-WMVFTS in the most of combinations of  $K$  and  $\kappa$  for all the accuracy metrics, but not significantly. Both embedding methods achieved similar performance. Therefore, our forecasting methods are equally good in most scenarios. However, the time spent to train the autoencoder has to be taken into account, since it is a neural network and it takes a considerable time to train and optimize the reconstruction error.

In contrast, in relation to SHWI-DS dataset, PCA-WMVFTS showed a superior performance than AE-WMVFTS in all the combinations of number of fuzzy sets and reduced dimensions. As the number of  $K$  dimensions and  $\kappa$  fuzzy sets increase, the difference between the methods decrease. Besides, our models presented optimal prediction results with a small number of reduced dimensions.

As mentioned before, in some experiments we changed the time resolution of the HPC-DS dataset, growing it to 30 minutes, then the accuracy metrics showed in Table 11 were calculated using this new sample rate. In opposi-

tion to other datasets, AE-WMVFTS presented smaller forecast error than PCA-WMVFTS on HPC-DS dataset for the most of combinations of  $K$  and  $\kappa$  considering the RMSE and MAE accuracy metrics. For MAPE and SMAPE, PCA-WMVFTS was better.

Therefore, both proposed models showed good results in both very high dimensional data, such as AEC-DS and SHWI-DS, and moderate dimensional data, such as HPC-DS, and PCA-WMVFTS is just slightly superior than AE-WMVFTS. Besides, we can improve the prediction performance of our models by just increasing a little the reduced dimensions, and  $\kappa$  equal 40 or 50 seems to be the optimal number of fuzzy sets.

### 5.2. $\gamma$ FTS versus Baseline models

In this subsection, we compare the forecast performance of our proposed models (PCA-WMVFTS, AE-WMVFTS and SOM-WMVFTS) with the baseline models. For all results presented here, the number of fuzzy sets  $\kappa$  was 50 and the number of  $K$  dimensions was 2 for our models, and the accuracy metrics were calculated in the testing set.

Table 12 presents the results of RMSE, MAE and MAPE for each baseline model on AEC-DS, as well as the accu-

Table 10: PCA-WMVFTS and AE-WMVFTS model performance with different number of K-dimensions (DIM) and fuzzy sets (FS) on SHWI-DS

PCA-WMVFTS					AE-WMVFTS				
DIM	FS	RMSE(Wh)	MAE(Wh)	MAPE(%)	SMAPE(%)	RMSE(Wh)	MAE(Wh)	MAPE(%)	SMAPE(%)
2	10	0.424	0.306	177.341	18.895	0.496	0.367	238.393	21.833
	20	0.31	0.188	83.209	12.102	0.387	0.262	145.92	16.811
	30	0.266	0.131	49.896	8.402	0.329	0.197	122.129	13.158
	40	0.193	0.087	33.955	5.882	0.259	0.14	96.22	9.39
	50	<b>0.169</b>	<b>0.062</b>	<b>17.823</b>	<b>4.285</b>	<b>0.221</b>	<b>0.106</b>	<b>32.536</b>	<b>7.178</b>
3	10	0.274	0.186	97.894	12.957	0.42	0.315	204.197	19.39
	20	0.143	0.056	15.844	4.173	0.235	0.123	127.802	8.38
	30	0.102	0.024	5.618	1.678	0.139	0.057	35.617	3.966
	40	0.055	0.012	2.549	0.845	0.095	0.029	7.355	2.024
	50	<b>0.04</b>	<b>0.008</b>	<b>1.451</b>	<b>0.482</b>	<b>0.049</b>	<b>0.015</b>	<b>3.735</b>	<b>1.117</b>
4	10	0.147	0.079	58.304	6.415	0.305	0.203	122.157	13.742
	20	0.045	0.013	3.597	1.035	0.119	0.053	14.55	3.635
	30	0.015	0.004	1.23	0.252	0.047	0.013	3.546	1
	40	0.006	0.003	0.338	0.11	0.023	0.006	0.902	0.322
	50	<b>0.003</b>	<b>0.003</b>	<b>0.259</b>	<b>0.076</b>	<b>0.012</b>	<b>0.004</b>	<b>0.565</b>	<b>0.199</b>
5	10	0.081	0.035	23.325	3.202	0.208	0.129	67.093	9.357
	20	0.012	0.005	0.879	0.306	0.052	0.017	3.522	1.195
	30	0.003	0.002	0.256	0.076	0.019	0.005	2.238	0.353
	40	0.001	0.002	0.208	0.055	0.004	0.003	0.309	0.097
	50	<b>0.0005</b>	<b>0.002</b>	<b>0.197</b>	<b>0.049</b>	<b>0.002</b>	<b>0.003</b>	<b>0.23</b>	<b>0.065</b>
6	10	0.045	0.017	5.267	1.562	0.159	0.08	28.949	5.847
	20	0.004	0.003	0.298	0.1	0.024	0.008	1.42	0.539
	30	0.001	0.002	0.195	0.048	0.005	0.002	0.336	0.115
	40	0.0005	0.002	0.191	0.046	0.003	0.003	0.23	0.063
	50	<b>0.0004</b>	<b>0.002</b>	<b>0.19</b>	<b>0.046</b>	<b>0.001</b>	<b>0.002</b>	<b>0.196</b>	<b>0.049</b>

Table 11: PCA-WMVFTS and AE-WMVFTS model performance with different number of K-dimensions (DIM) and fuzzy sets (FS) on HPC-DS

PCA-WMVFTS					AE-WMVFTS				
DIM	FS	RMSE(Wh)	MAE(Wh)	MAP (%)	SMAPE(%)	RMSE(Wh)	MAE(Wh)	MAPE(%)	SMAPE(%)
2	10	0.549	0.418	88.727	24.827	0.507	0.386	93.654	25.476
	20	0.511	0.355	56.347	17.858	0.383	0.268	60.252	19.274
	30	0.469	0.297	51.887	15.694	0.34	0.232	51.57	17.037
	40	0.41	0.245	43.124	13.525	0.324	0.218	48.976	16.253
	50	<b>0.366</b>	<b>0.204</b>	<b>37.303</b>	<b>11.529</b>	<b>0.304</b>	<b>0.206</b>	<b>46.722</b>	<b>15.533</b>
3	10	0.517	0.374	78.947	22.804	0.451	0.359	92.251	24.938
	20	0.368	0.24	42.782	13.813	0.32	0.23	57.631	17.769
	30	0.276	0.155	31.755	10.163	0.268	0.186	47.405	15.246
	40	0.204	0.108	22.335	7.564	0.245	0.158	40.042	13.104
	50	<b>0.162</b>	<b>0.079</b>	<b>17.528</b>	<b>5.807</b>	<b>0.227</b>	<b>0.137</b>	<b>37.023</b>	<b>11.837</b>
4	10	0.421	0.309	70.581	20.532	0.398	0.325	90.238	24.065
	20	0.236	0.147	28.93	9.689	0.257	0.186	51.104	15.894
	30	0.138	0.071	15.501	5.438	0.217	0.143	41.447	13.013
	40	0.084	0.039	8.63	3.147	0.201	0.116	33.966	10.828
	50	<b>0.061</b>	<b>0.023</b>	<b>5.24</b>	<b>1.941</b>	<b>0.182</b>	<b>0.098</b>	<b>30.187</b>	<b>9.548</b>

racy metrics results for PCA-WMVFTS, AE-WMVFTS and SOM-WMVFTS proposed models.

Table 12: Models performance on AEC-DS dataset

Method	RMSE(Wh)	MAE(Wh)	MAPE(%)
Persistence	64.749	29.107	24.828
SARIMAX	172.283	139.15	195.942
PCA-SARIMAX	158.768	124.465	170.801
LSTM	71.329	42.59	44.748
<b>PCA-WMVFTS</b>	<b>5.456</b>	<b>2.05</b>	<b>1.758</b>
<b>AE-WMVFTS</b>	<b>5.516</b>	<b>2.493</b>	<b>2.405</b>
<b>SOM-WMVFTS</b>	<b>18.292</b>	<b>7.498</b>	<b>4.503</b>

Comparing the results with those obtained by baseline models, it is clear that PCA-WMVFTS, AE-WMVFTS, and SOM-WMVFTS outperform them. Among our forecasting models, SOM-WMVFTS presented the worst performance and PCA-WMVFTS showed the smallest error, but PCA-WMVFTS is just slightly superior than AE-WMVFTS. A deep learning model such as LSTM presented a performance worse than Persistence, which was the best model among the baseline models.

Table 13 shows the accuracy for the baseline models and our proposed models on HPC-DS. We changed the time resolution of this dataset to 30 minutes, then these error metrics present the models performance for this new sample rate.

Table 13: Models performance on HPC-DS dataset

Method	RMSE(kW)	MAE(kW)	MAPE(%)
Persistence	0.898	0.514	63.793
SARIMAX	0.901	0.517	64.984
PCA-SARIMAX	0.901	0.517	64.944
LSTM	0.122	0.088	17.49
<b>PCA-WMVFTS</b>	<b>0.366</b>	<b>0.204</b>	<b>37.303</b>
<b>AE-WMVFTS</b>	<b>0.304</b>	<b>0.206</b>	<b>46.722</b>
<b>SOM-WMVFTS</b>	<b>0.415</b>	<b>0.256</b>	<b>48.397</b>

In contrast of AEC-DS, the LSTM showed the smallest prediction error compared to all models. In this dataset the performance of our models was worse than LSTM, however, as presented on Table 11, we can improve our model by just increasing the embedding dimension or the number of fuzzy sets, then our proposed models may be better than LSTM. Among our models, AE-WMVFTS achieved the smallest prediction error and SOM-WMVFTS the highest.

As shown on Table 14, our proposed methods is much superior than baseline models on SHWI-DS dataset. PCA-WMVFTS presented the smallest error compared to all forecasting models. SOM-WMVFTS showed again the highest error among our models, and the best baseline

Table 14: Models performance on SHWI-DS dataset

Method	RMSE(kW)	MAE(kW)	MAPE(%)
Persistence	0.846	0.468	251.68
SARIMAX	1.298	0.719	284.08
PCA-SARIMAX	0.994	0.577	272.337
LSTM	0.594	0.338	129.681
<b>PCA-WMVFTS</b>	<b>0.169</b>	<b>0.062</b>	<b>17.823</b>
<b>AE-WMVFTS</b>	<b>0.221</b>	<b>0.106</b>	<b>32.536</b>
<b>SOM-WMVFTS</b>	<b>0.389</b>	<b>0.211</b>	<b>92.529</b>

model was LSTM.

Table 15 shows the skill score of PCA-WMVFTS, AE-WMVFTS and SOM-WMVFTS with respect to some baseline models. The accuracy metric selected was the RMSE.

PCA-WMVFTS presented an improvement in RMSE greater than 90% with respect to all baseline models on AEC-DS. In relation to SHWI-DS, the improvement is greater than 80% with respect to persistence, SARIMAX and PCA-SARIMAX models, and PCA-WMVFTS showed an enhancement of 71% compared to LSTM, which was the best model among baseline models. In regard to HPC-DS, PCA-WMVFTS is 66% worse than LSTM and presented an enhancement by 59% with respect the other baseline models.

AE-WMVFTS also showed an enhancement in RMSE greater than 90% with respect to all baseline models on AEC-DS. In regard to SHWI-DS dataset, AE-WMVFTS presented a rise in RMSE 74% with respect to Persistence model and it had an improvement by 83% and 78% with respect to SARIMAX and PCA-SARIMAX, respectively. Compared to LSTM, AE-WMVFTS has an improvement in RMSE by 63% on SHWI-DS. In contrast, AE-WMVFTS is 59% worse than LSTM on HPC-DS data, but it presents an improvement by 66% with respect to the other baseline models.

SOM-WMVFTS presented an improvement in RMSE by 89%, 88%, 74% and 72% with respect to SARIMAX, PCA-SARIMAX, Persistence and LSTM on AEC-DS, respectively. In relation to HPC-DS, SOM-WMVFTS showed a deterioration by 70% with respect to LSTM and an enhancement by 54% with respect to other baseline models. In regard to SHWI-DS, SOM-WMVFTS had an enhancement by 35% compared to LSTM and it presented an increase in RMSE by 70%, 61% and 54% with respect to SARIMAX, PCA-SARIMAX and Persistence, respectively.

Although our forecast models presented a negative skill score with respect to LSTM on HPC-DS, we can raise its prediction performance by just growing the number of reduced dimensions or the number of fuzzy sets. Besides, LSTM may take a considerable time to train and optimize.

It can be seen from the results above that, compared to baseline models, PCA-WMVFTS, AE-WMVFTS and

Table 15: Skill score of PCA-WMVFTS, AE-WMVFTS and SOM-WMVFTS with respect to baseline models

	PCA-WMVFTS			AE-WMVFTS			SOM-WMVFTS		
	AEC-DS	HPC-DS	SHWI-DS	AEC-DS	HPC-DS	SHWI-DS	AEC-DS	HPC-DS	SHWI-DS
Persistence	0.92	0.59	0.80	0.91	0.66	0.74	0.72	0.54	0.54
SARIMAX	0.97	0.59	0.87	0.97	0.66	0.83	0.89	0.54	0.70
PCA-SARIMAX	0.97	0.59	0.83	0.97	0.66	0.78	0.88	0.54	0.61
LSTM	0.92	-2.00	0.72	0.92	-1.49	0.63	0.74	-2.40	0.35

SOM-WMVFTS achieve optimal prediction performance on all datasets. The proposed models presented better results on AEC-DS and SHWI-DS, showing that they output good results in both very high dimensional data, such as AEC-DS and SHWI-DS, and moderate dimensional data, such as HPC-DS.

### 5.3. $\gamma$ FTS versus Competitors models

In this subsection, we compare the performance of the proposed models with several state-of-the-art forecasting models proposed in the literature (i.e. competitors models). It is worth noting that each one of these models used a different experimental methodology, either in terms of cross-validation methodology or train/test split. In those terms, it is counterproductive to perform a different experimental set up for each competitor model and this research used their published results as they are, to compare with our experimental results.

Table 16 shows the results of RMSE, MAE and MAPE for several state-of-the-art forecasting models proposed in the literature tested on AEC-DS with all the features and feature selection, as well as the accuracy metrics results for our proposed models. The accuracy metrics were calculated in the testing set.

Table 16: Models performance on AEC-DS dataset (FS = feature selection)

Method	RMSE(Wh)	MAE(Wh)	MAPE(%)
GBM [19]	66.65	35.22	38.29
GBM (FS) [19]	66.21	35.24	38.65
MLP [20]	66.29	29.55	27.96
MPL (FS) [20]	59.84	27.28	27.09
CNN-GRU [23]	31	24	-
HSBUFC [21]	5.44	4.45	2
AIS-RNN [25]	59.81	23.42	18.84
<b>PCA-WMVFTS</b>	<b>5.456</b>	<b>2.05</b>	<b>1.758</b>
<b>AE-WMVFTS</b>	<b>5.516</b>	<b>2.493</b>	<b>2.405</b>
<b>SOM-WMVFTS</b>	<b>18.292</b>	<b>7.498</b>	<b>11.059</b>

According to Table 16, PCA-WMVFTS is superior than all competitors models with RMSE of 5.456 Wh, a MAE

of 2.05 and a MAPE of 1.758%. AE-WMVFTS showed a high performance compared to GBM, MPL, CNN-GRU and AIS-RNN and an accuracy error quite similar to HSBUFC. SOM-WMVFTS is inferior than HSBUFC, but it is superior than other competitors models.

The best model among the competitors model was HSBUFC, which showed a MAE and MAPE higher than PCA-WMVFTS and a RMSE equivalent to our model. HSBUFC is just slightly superior than AE-WMVFTS taking into account RMSE and MAPE. In contrast, SOM-WMVFTS presented a performance worse than HSBUFC in all accuracy metrics.

Table 17 presents the accuracy for the competitors models and our models on HPC-DS. In these experiments, the time resolution of the dataset was the original one, in other words, sample rate equal one minute. PCA-WMVFTS, AE-WMVFTS and SOM-WMVFTS are inferior than HSBUFC, but our forecast models outperform the other competitors models.

Table 17: Models performance on HPC-DS dataset

Method	RMSE(kW)	MAE(kW)	MAPE(%)
CNN-LSTM [22]	0.611	0.373	34.84
M-BDLSTM [24]	0.565	0.346	29.1
CNN-GRU [23]	0.47	0.33	-
HSBUFC [21]	0.029	0.022	3.71
<b>PCA-WMVFTS</b>	<b>0.103</b>	<b>0.053</b>	<b>8.815</b>
<b>AE-WMVFTS</b>	<b>0.092</b>	<b>0.054</b>	<b>11.668</b>
<b>SOM-WMVFTS</b>	<b>0.095</b>	<b>0.049</b>	<b>9.671</b>

Tables 18 and 19 show the skill score of PCA-WMVFTS, AE-WMVFTS and SOM-WMVFTS with respect to some competitors models tested on AEC-DS and HPC-DS data sets, respectively. The accuracy metric selected was the RMSE.

In relation to AEC-DS, the methods PCA-WMVFTS and AE-WMVFTS presented an improvement in RMSE greater than 90% with respect to GBM, MLP and AIS-RNN forecast models. Both PCA-WMVFTS and AE-WMVFTS are 82% better than CNN-GRU. Compared to HSBUFC, AE-WMVFTS had a deterioration by just

Table 18: Skill score of PCA-WMVFTS, AE-WMVFTS and SOM-WMVFTS with respect to competitors models on AEC-DS

	PCA-WMVFTS	AE-WMVFTS	SOM-WMVFTS
GBM (FS)	0.92	0.92	0.72
MPL (FS)	0.91	0.91	0.69
CNN-GRU	0.82	0.82	0.41
HSBUFC	0.00	-0.01	-2.36
AIS-RNN	0.91	0.91	0.69

Table 19: Skill score of PCA-WMVFTS, AE-WMVFTS and SOM-WMVFTS with respect to competitors models on HPC-DS

	PCA-WMVFTS	AE-WMVFTS	SOM-WMVFTS
CNN-LSTM	0.83	0.85	0.84
M-BDLSTM	0.82	0.84	0.83
CNN-GRU	0.78	0.80	0.80
HSBUFC	-2.55	-2.17	-2.28

1.38% and PCA-WMVFTS is equivalent to HSBUFC. SOM-WMVFTS had an enhancement in RMSE by 72%, 0.69 and 0.41% with respect to GBM, MLP, AIS-RNN and CNN-GRU, respectively. However, SOM-WMVFTS is 70% worse than HSBUFC.

In regard to HPC-DS dataset, our three proposed models showed an improvement in RMSE with respect to the CNN-LSTM, M-BDLSTM and CNN-GRU models. AE-WMVFTS and SOM-WMVFTS had an enhancement greater than 80% compared to these competitors models. PCA-WMVFTS is 78% better than CNN-GRU and presented an enhancement greater than 80% with respect to CNN-LSTM and M-BDLSTM. In contrast, compared to HSBUFC, our approach with two-dimensional embedding and 50 fuzzy sets showed a deterioration around 70%.

Although our models showed a negative skill score with respect to HSBUFC, we can raise their prediction performance by just growing the number of reduced dimensions or the number of fuzzy sets. Additionally, HSBUFC is a deep learning model that may take a considerable time to train and optimize, while FTS models are very fast to train.

It can be concluded that our three proposed methods with 2 reduced dimensions and 50 fuzzy sets significantly outperformed several competitors models, outputting a consistent and accurate prediction, since the methods presented equally good results in all the data sets that were used, reinforcing the model’s capacity to make excellent predictions for different data.

#### 5.4. Analysis and Discussion

This section aims to discuss the accuracy, parsimony, computational cost and explainability of  $\gamma$ FTS models con-

sidering the results of the experiments.

As a rule of thumb, increasing the embedding dimension and the number of fuzzy sets increase the accuracy of  $\gamma$ FTS models, except for the SOM function. However, there is a clear trade-off: increasing these hyperparameters improves accuracy but decreases the parsimony and explainability.

The parsimony, or complexity, is intended to be minimized once it means the number of parameters or rules of the model. As the model complexity increases also its computational cost and training time increase. This is relevant in the domain of IoE applications, since these models can be embedded in edge devices with low computational power.  $\gamma$ FTS models are less parsimonious than SARIMAX but way more parsimonious, for instance, than deep learning models such as LSTM and CNN.

It is also worth observing that the broad class of FTS models are data-driven and white-box models that are easy to explain and audit, a feature that gained high importance in recent years.  $\gamma$ FTS models have their explainability affected by two factors: the embedding function and the number of fuzzy sets. The most impacting factor is the number of fuzzy sets which automatically increases the number of rules and makes the model more complex. The embedding function is not a complex issue per se, since the presented functions are all invertible, and the values of the fuzzy sets can be converted back to values of the original data space.

Future investigations may also focus on the properties of the feature spaces of each embedding function. It is important to note that the PCA, which is a linear embedding, in general, performed better than AE and SOM, which are nonlinear embeddings. The less accurate embedding in general was the SOM, and a possible hypothesis for this is due to their discrete embedding space, but it is exactly this property that makes it more explainable due to the easiness to identify features in the embedded space.

In this work, the proposed approach aims to address the smart building energy consumption forecasting problem. The embedding algorithm is used to extract the main information that better represent the content of multivariate time series for the subsequent energy forecasting task. PCA, autoencoder and SOM algorithms can be used to identify the most relevant information on the smart buildings datasets based on available historical data.

## 6. Conclusions and Future Works

In this work, we investigated the possible benefits provided by a method that combines embedding transformation and fuzzy time series forecasting approach for tackling the high-dimensional time series forecasting problem. We proposed a new methodology (namely  $\gamma$ FTS) for handling high-dimensional data, applying data embedding transformation and FTS model in the low-dimensional learned representation space.



Since each variable  $\mathcal{V}$  depends not only on its historic values but also of several contemporaneous variables, it is mandatory to select a set of suitable variables as input. In this sense, the embedding techniques allow us to extract and exploit a new feature space that better represents the inherent complexity of multivariate time series, also mitigating collinearity phenomena and catching latent interactions among features.

High dimensional time series are a big challenge for forecasting methods. Statistical models can suffer from the curse of dimensionality and multi-collinearity, and the existing fuzzy time series models can be unfeasible if all features were used to train the model. On the positive side, the flexibility, simplicity, readability and accuracy of FTS methods make this approach interesting for many IoE applications.

The proposed approach aimed to address the energy consumption forecasting problem in smart buildings. The PCA, autoencoder and SOM algorithms were used to extract new feature space that better represents the content of energy consumption multivariate time series for the subsequent forecasting task. The embedding methods allow us to extract the relevant information that supports the target variable forecasting.

Computational experiments were performed to assess the accuracy of  $\gamma$ FTS against some baseline models (persistence, SARIMAX, PCA-SARIMAX and LSTM) and state-of-the-art machine learning and deep learning models recently proposed in the literature.

Our experimental evaluation showed that, compared to other energy consumption forecasting methods,  $\gamma$ FTS achieves the best prediction performance on smart building energy consumption problem. Therefore, our approach has a great value in smart building and IoE applications, and can help homeowners reduce their power consumption and provide better energy-saving strategies.

Besides, the proposed methodology generates forecasting models readable and explainable and their accuracy are controlled basically by two parameters: the partitioning of the target variable (number of fuzzy sets) and the embedding dimension  $K$ . As the number of reduced dimensions and fuzzy sets increase, the forecast error decreases, then we can improve our approach by just increasing these two hyperparameters when needed.

As future work, we intend to extend the proposed methods to handle multivariate non-stationary time series and the implementation of a MIMO (multiple input multiple output) and many step-ahead forecasting approach.

## References

- [1] I. T. Union, *Itu internet report 2005: The internet of things (2005)*.
- [2] J. Gubbi, R. Buyya, S. Marusic, M. Palaniswami, *Internet of things (iot): A vision, architectural elements, and future directions*, *Future Gener. Comput. Syst.* 29 (7) (2013) 1645–1660. doi:10.1016/j.future.2013.01.010. URL <https://doi.org/10.1016/j.future.2013.01.010>
- [3] D. Miorandi, S. Sicari, F. De Pellegrini, I. Chlamtac, *Internet of things: Vision, applications and research challenges*, *Ad Hoc Networks* 10 (7) (2012) 1497–1516. doi:<https://doi.org/10.1016/j.adhoc.2012.02.016>. URL <https://www.sciencedirect.com/science/article/pii/S1570870512000674>
- [4] S. Reka, *Future effectual role of energy delivery: A comprehensive review of internet of things and smart grid, Renewable and Sustainable Energy Reviews* 91 (04 2018). doi:10.1016/j.rser.2018.03.089.
- [5] Y. Shahzad, H. Javed, H. Farman, J. Ahmad, B. Jan, M. Zubair, *Internet of energy: Opportunities, applications, architectures and challenges in smart industries*, *Comput. Electr. Eng.* 86 (2020) 106739. doi:10.1016/j.compeleceng.2020.106739. URL <https://doi.org/10.1016/j.compeleceng.2020.106739>
- [6] M. Nitti, V. Pilloni, G. Colistra, L. Atzori, *The virtual object as a major element of the internet of things: A survey*, *IEEE Commun. Surv. Tutorials* 18 (2) (2016) 1228–1240. doi:10.1109/COMST.2015.2498304. URL <https://doi.org/10.1109/COMST.2015.2498304>
- [7] M. Jaradat, M. H. A. Jarrah, A. Bousselham, Y. Jararweh, M. Al-Ayyoub, *The internet of energy: Smart sensor networks and big data management for smart grid*, in: *The 10th International Conference on Future Networks and Communications (FNC 2015) / The 12th International Conference on Mobile Systems and Pervasive Computing (MobiSPC 2015) / Affiliated Workshops*, August 17–20, 2015, Belfort, France, Vol. 56 of *Procedia Computer Science*, Elsevier, 2015, pp. 592–597. doi:10.1016/j.procs.2015.07.250. URL <https://doi.org/10.1016/j.procs.2015.07.250>
- [8] H. Shahinzadeh, J. Moradi, G. B. Gharehpetian, H. Nafisi, M. Abedi, *Internet of energy (ioe) in smart power systems*, 2019, pp. 627–636. doi:10.1109/KBEI.2019.8735086.
- [9] M. Jaradat, M. Jarrah, A. Bousselham, Y. Jararweh, M. Al-Ayyoub, *The internet of energy: Smart sensor networks and big data management for smart grid*, *Procedia Computer Science* 56 (2015) 592–597. doi:10.1016/j.procs.2015.07.250. URL <https://doi.org/10.1016/j.procs.2015.07.250>
- [10] G. Lobaccaro, S. Carlucci, E. Löfström, *A review of systems and technologies for smart homes and smart grids*, *Energies* 9 (5) (2016). doi:10.3390/en9050348. URL <https://www.mdpi.com/1996-1073/9/5/348>
- [11] M. Manic, K. Amarasinghe, J. J. Rodriguez-Andina, C. Rieger, *Intelligent buildings of the future: Cyberaware, deep learning powered, and human interacting*, *IEEE Industrial Electronics Magazine* 10 (4) (2016) 32–49. doi:10.1109/MIE.2016.2615575.
- [12] Z. Hammami, M. Sayed Mouchaweh, W. Mouelhi, L. B. Said, *Neural networks for online learning of non-stationary data streams: a review and application for smart grids flexibility improvement*, *Artif. Intell. Rev.* 53 (8) (2020) 6111–6154. doi:10.1007/s10462-020-09844-3. URL <https://doi.org/10.1007/s10462-020-09844-3>
- [13] M. Mohammadi, A. Al-Fuqaha, S. Sorour, M. Guizani, *Deep learning for iot big data and streaming analytics: A survey*, *IEEE Communications Surveys Tutorials* 20 (4) (2018) 2923–2960. doi:10.1109/COMST.2018.2844341.
- [14] P. C. de Lima Silva, P. de Oliveira e Lucas, H. J. Sadaei, F. G. Guimarães, *Distributed evolutionary hyperparameter optimization for fuzzy time series*, *IEEE Trans. Netw. Serv. Manag.* 17 (3) (2020) 1309–1321. doi:10.1109/TNSM.2020.2980289. URL <https://doi.org/10.1109/TNSM.2020.2980289>
- [15] P. C. de Lima Silva, C. A. S. Junior, M. A. Alves, R. Silva, M. Weiss-Cohen, F. G. Guimarães, *Forecasting in non-stationary environments with fuzzy time series*, *Applied Soft Computing* 97 (Part B) (2020) 106825. doi:10.1016/j.asoc.2020.106825. URL <https://doi.org/10.1016/j.asoc.2020.106825>
- [16] A. Zheng, J. Jamelipour, *Wireless Sensor Networks: A Networking Perspective*, Wiley-IEEE Press, 2009.
- [17] M. A. M. Vieira, J. Coelho, Claudionor N., J. da Silva, Diógenes.Cecílio., J. da Mata, *Survey on wireless sensor net-*

- work devices, in: IEEE Conference on Emerging Technologies and Factory Automation (ETFA), 2003, Vol. 1, 2003, pp. 537 – 544 vol.1. doi:10.1109/ETFA.2003.1247753.
- [18] E. Mocanu, P. H. Nguyen, M. Gibescu, W. L. Kling, Deep learning for estimating building energy consumption, *Sustainable Energy, Grids and Networks* 6 (2016) 91–99. doi:https://doi.org/10.1016/j.segan.2016.02.005. URL https://www.sciencedirect.com/science/article/pii/S2352467716000163
- [19] L. M. Candanedo, V. Feldheim, D. Deramaix, Data driven prediction models of energy use of appliances in a low-energy house, *Energy and Buildings* 140 (2017) 81–97. doi:https://doi.org/10.1016/j.enbuild.2017.01.083. URL https://www.sciencedirect.com/science/article/pii/S0378778816308970
- [20] M. Chammas, A. Makhoul, J. Demerjian, An efficient data model for energy prediction using wireless sensors, *Comput. Electr. Eng.* 76 (2019) 249–257. doi:10.1016/j.compeleceng.2019.04.002. URL https://doi.org/10.1016/j.compeleceng.2019.04.002
- [21] D. Syed, H. Abu-Rub, A. Ghayeb, S. S. Refaat, Household-level energy forecasting in smart buildings using a novel hybrid deep learning model, *IEEE Access* 9 (2021) 33498–33511. doi:10.1109/ACCESS.2021.3061370.
- [22] T.-Y. Kim, S.-B. Cho, Predicting residential energy consumption using cnn-lstm neural networks, *Energy* 182 (2019) 72–81. doi:https://doi.org/10.1016/j.energy.2019.05.230. URL https://www.sciencedirect.com/science/article/pii/S0360544219311223
- [23] M. Sajjad, Z. A. Khan, A. Ullah, T. Hussain, W. Ullah, M. Y. Lee, S. W. Baik, A novel cnn-gru-based hybrid approach for short-term residential load forecasting, *IEEE Access* 8 (2020) 143759–143768. doi:10.1109/ACCESS.2020.3009537.
- [24] F. U. M. Ullah, A. Ullah, I. U. Haq, S. Rho, S. W. Baik, Short-term prediction of residential power energy consumption via cnn and multi-layer bi-directional lstm networks, *IEEE Access* 8 (2020) 123369–123380. doi:10.1109/ACCESS.2019.2963045.
- [25] L. Munkhdalai, T. Munkhdalai, K. H. Park, T. Amarbayasgalan, E. Batbaatar, H. W. Park, K. H. Ryu, An end-to-end adaptive input selection with dynamic weights for forecasting multivariate time series, *IEEE Access* 7 (2019) 99099–99114. doi:10.1109/ACCESS.2019.2930069.
- [26] T. Parhizkar, E. Rafiepour, A. Parhizkar, Evaluation and improvement of energy consumption prediction models using principal component analysis based feature reduction, *Journal of Cleaner Production* 279 (2021) 123866. doi:https://doi.org/10.1016/j.jclepro.2020.123866. URL https://www.sciencedirect.com/science/article/pii/S0959652620339111
- [27] Q. Song, B. S. Chissom, Fuzzy time series and its models, *Fuzzy Sets and Systems* 54 (3) (1993) 269–277. doi:https://doi.org/10.1016/0165-0114(93)90372-0. URL https://www.sciencedirect.com/science/article/pii/0165011493903720
- [28] K. P. F.R.S., Liii. on lines and planes of closest fit to systems of points in space, *The London, Edinburgh, and Dublin Philosophical Magazine and Journal of Science* 2 (11) (1901) 559–572. doi:10.1080/14786440109462720.
- [29] D. E. Rumelhart, G. E. Hinton, R. J. Williams, Learning internal representations by error propagation, in: D. E. Rumelhart, J. L. McClelland (Eds.), *Parallel Distributed Processing: Explorations in the Microstructure of Cognition, Volume 1: Foundations*, MIT Press, Cambridge, MA, 1986, pp. 318–362.
- [30] T. Kohonen, *Self-Organizing Maps*, Third Edition, Springer Series in Information Sciences, Springer, 2001. doi:10.1007/978-3-642-56927-2. URL https://doi.org/10.1007/978-3-642-56927-2
- [31] M. C. dos Santos, F. G. Guimarães, P. C. d. L. Silva, High-dimensional multivariate time series forecasting using self-organizing maps and fuzzy time series, in: 2021 IEEE International Conference on Fuzzy Systems (FUZZ-IEEE), 2021, pp. 1–6. doi:10.1109/FUZZ45933.2021.9494496.
- [32] H. V. Bitencourt, F. G. Guimarães, High-dimensional multivariate time series forecasting in iot applications using embedding non-stationary fuzzy time series, *CoRR abs/2107.09785* (2021). arXiv:2107.09785. URL https://arxiv.org/abs/2107.09785
- [33] A. Gensler, J. Henze, B. Sick, N. Raabe, Deep learning for solar power forecasting - an approach using autoencoder and lstm neural networks, in: 2016 IEEE International Conference on Systems, Man, and Cybernetics (SMC), 2016, pp. 002858–002865. doi:10.1109/SMC.2016.7844673.
- [34] P. C. de Lima Silva, e Patrícia de Oliveira e Lucas, F. G. Guimarães, A distributed algorithm for scalable fuzzy time series, in: *International Conference on Green, Pervasive, and Cloud Computing*, Springer, 2019, pp. 42–56. doi:10.1007/978-3-030-19223-5\_4. URL https://doi.org/10.1007/978-3-030-19223-5\_4
- [35] D. Dua, C. Graff, UCI machine learning repository (2017). URL http://archive.ics.uci.edu/ml
- [36] Kaggle, Smart home dataset with weather information, https://www.kaggle.com/taranvee/smart-home-dataset-with-weather-information, accessed on 28 Ago 2021 (2021).
- [37] C. Voyant, G. Notton, S. Kalogirou, M.-L. Nivet, C. Paoli, F. Motte, A. Foulloy, Machine learning methods for solar radiation forecasting: A review, *Renewable Energy* 105 (2017) 569 – 582. doi:https://doi.org/10.1016/j.renene.2016.12.095. URL http://www.sciencedirect.com/science/article/pii/S0960148116311648
- [38] T. G. Smith, et al., pmdarima: Arima estimators for Python, [Online; accessed jtoday]. URL http://www.alkaline-ml.com/pmdarima
- [39] S. Hochreiter, J. Schmidhuber, Long short-term memory, *Neural computation* 9 (8) (1997) 1735–1780.
- [40] J. Bergstra, D. Yamins, D. Cox, Making a science of model search: Hyperparameter optimization in hundreds of dimensions for vision architectures (2013) 115–123.
- [41] P. C. d. L. Silva, pyfts : Fuzzy time series for python (03 2016). doi:10.5281/zenodo.597359.
- [42] F. Pedregosa, G. Varoquaux, A. Gramfort, V. Michel, B. Thirion, O. Grisel, M. Blondel, P. Prettenhofer, R. Weiss, V. Dubourg, J. Vanderplas, A. Passos, D. Cournapeau, M. Brucher, M. Perrot, E. Duchesnay, Scikit-learn: Machine learning in Python, *Journal of Machine Learning Research* 12 (2011) 2825–2830.
- [43] F. Chollet, et al., Keras, https://keras.io (2015).
- [44] M. Abadi, A. Agarwal, P. Barham, E. Brevdo, Z. Chen, C. Citro, G. S. Corrado, A. Davis, J. Dean, M. Devin, S. Ghemawat, I. Goodfellow, A. Harp, G. Irving, M. Isard, Y. Jia, R. Jozefowicz, L. Kaiser, M. Kudlur, J. Levenberg, D. Mané, R. Monga, S. Moore, D. Murray, C. Olah, M. Schuster, J. Shlens, B. Steiner, I. Sutskever, K. Talwar, P. Tucker, V. Vanhoucke, V. Vasudevan, F. Viégas, O. Vinyals, P. Warden, M. Wattenberg, M. Wicke, Y. Yu, X. Zheng, TensorFlow: Large-scale machine learning on heterogeneous systems, software available from tensorflow.org (2015). URL https://www.tensorflow.org/
- [45] S. Seabold, J. Perktold, statsmodels: Econometric and statistical modeling with python, in: 9th Python in Science Conference, 2010.